CELLULAR LOGISTICS
2016, VOL. 6, NO. 3, e1228791 (13 pages)
http://dx.doi.org/10.1080/21592799.2016.1228791

Taylor & Francis
Taylor & Francis Group

RESEARCH PAPER

OPEN ACCESS

Neo1 and phosphatidylethanolamine contribute to vacuole membrane fusion in *Saccharomyces cerevisiae*

Yuantai Wu, Mehmet Takar, Andrea A. Cuentas-Condori, and Todd R. Graham

Department of Biological Sciences, Vanderbilt University, Nashville, TN, USA

ABSTRACT

NEO1 is an essential gene in budding yeast and belongs to a highly conserved subfamily of P-type ATPase genes that encode phospholipid flippases. Inactivation of temperature sensitive *neo1*^{ts} alleles produces pleiomorphic defects in the secretory and endocytic pathways, including fragmented vacuoles. A screen for multicopy suppressors of *neo1-2*^{ts} growth defects yielded *YPT7*, which encodes a Rab7 homolog involved in SNARE-dependent vacuolar fusion. *YPT7* suppressed the vacuole fragmentation phenotype of *neo1-2*, but did not suppress Golgi-associated protein trafficking defects. Neo1 localizes to Golgi and endosomal membranes and was only observed in the vacuole membrane, where Ypt7 localizes, in retromer mutants or when highly overexpressed in wild-type cells. Phosphatidylethanolamine (PE) has been implicated in Ypt7-dependent vacuolar membrane fusion *in vitro* and is a potential transport substrate of Neo1. Strains deficient in PE synthesis (*psd1Δ psd2Δ*) displayed fragmented vacuoles and the *neo1-2* fragmented vacuole phenotype was also suppressed by overexpression of *PSD2*, encoding a phosphatidylserine decarboxylase that produces PE at endosomes. In contrast, *neo1-2* was not suppressed by overexpression of *VPS39*, an effector of Ypt7 that forms a membrane contact site potentially involved in PE transfer between vacuoles and mitochondria. These results support the crucial role of PE in vacuole membrane fusion and implicate Neo1 in concentrating PE in the cytosolic leaflet of Golgi and endosomes, and ultimately the vacuole membrane.

ARTICLE HISTORY
Received 20 June 2016
Revised 5 August 2016
Accepted 19 August 2016

KEYWORDS
flippase; membrane asymmetry; P4-ATPase; Rab protein; SNARE; vacuoles; Ypt7

Introduction

Biological membranes are an assembly of protein and lipid molecules organized into a bilayer structure with 2 distinct surfaces. Integral membrane proteins are intrinsically asymmetric and display functionally unique domains on opposite sides of the membrane. The phospholipid composition of the 2 leaflets of a membrane can also be very different and this transverse asymmetry has substantial physiological implications for the membrane system.[1,2] Lipid molecules enriched on the cytosolic leaflet of the plasma membrane include phosphatidylserine (PS), phosphatidylethanolamine (PE), phosphatidylinositol and phosphoinositides, whereas sphingolipids, glycosphingolipids and phosphatidylcholine are typically enriched in the extracellular leaflet.[3] Phospholipid asymmetry is crucial for recruitment of specific peripheral membrane proteins and the function of numerous transporters and channels within the membrane. Thus, the appropriate asymmetric organization is important for many membrane-centered processes, including signal transduction, cell motility, cell polarity, cell division, vesicular transport and transport of ions and other molecules across the bilayer.[1]

Phospholipid asymmetry is controlled by flippases, floppases and scramblases; proteins that facilitate interleaflet transport of phospholipid molecules. The type IV P-type ATPases (P4-ATPases) catalyze a unidirectional, ATP-dependent, *i*nward fl*i*p of specific phospholipid species from the extracellular leaflet of the plasma membrane to the cytosolic leaflet (fl*i*ppase activity).[4,5] PS and PE are common substrates of P4-ATPases, which appear to be primarily responsible for establishing the asymmetric distribution of these aminophospholipids in the cytosolic leaflet.[6] ABC transporters in the multidrug resistance (MDR) family can catalyze *o*utward fl*o*p of phospholipids from the cytosolic leaflet to the extracellular leaflet (fl*o*ppase activity), but often with less headgroup specificity as compared to the flippase activity catalyzed by the P4-ATPases.[7] The combined activities of the flippases and floppases set the asymmetric membrane structure, which can be rapidly dissolved by activation of a scramblase.[8] TMEM16F and Xkr8 appear to be the scramblases responsible for the regulated exposure of PS in the extracellular leaflet of the plasma membrane required for blood clotting reactions and recognition of apoptotic cells, respectively.[9,10]

The asymmetric phospholipid organization of the plasma membrane and its physiological significance is becoming clear; however, less is known about how the membrane organization of intracellular organelles influences their function. Eukaryotic cells typically express multiple P4-ATPases and many of these flippases reside within Golgi and endosomal membranes.[2] For

CONTACT Todd R. Graham tr.graham@vanderbilt.edu VU Station B, Box 35-1634N, Nashville, TN 37235, USA.
Supplemental data for this article can be accessed on the publisher's website.

example, the budding yeast *Saccharomyces cerevisiae* expresses 5 P4-ATPases; Drs2, Neo1, Dnf1, Dnf2 and Dnf3.[11] Only Dnf1 and Dnf2 are present on the plasma membrane of growing cells, although these P4-ATPases also localize to Golgi and endosomal membranes.[11] Drs2 and Dnf3 localize primarily to the *trans*-Golgi network and Neo1 appears to be broadly distributed through the Golgi and endosomal system.[11-14] As membrane flows rapidly by vesicular transport between the Golgi, plasma membrane, endosomes and vacuole, the activity of a P4-ATPase in the Golgi should influence the organization of all of these membranes. ATP9A and ATP9B, the mammalian orthologs of Neo1, also localize to Golgi and endosomal membranes.[15] In contrast, TAT-5 in *Caenorhabditis elegans* (Neo1 ortholog) is reported to localize to the plasma membrane and inactivation of *TAT-5* leads to the specific exposure of PE in the plasma membrane outer leaflet.[16] This result suggests that PE could be the primary substrate of Neo1/TAT-5/ATP9 subgroup of P4-ATPases, although none of these proteins have been purified and assayed in a reconstituted system to clearly define their substrate preferences.

To better understand why *NEO1* is an essential gene in budding yeast, several temperature-sensitive (ts) alleles of *neo1* have been recovered and used to analyze the cellular consequences of acutely inactivating Neo1 function.[12,14] The phenotypes observed are pleiomorphic and include defects in COPI-dependent protein transport from the Golgi to the ER, defects in GGA/clathrin-dependent protein transport from the ER to late endosome, and exposure of both PS and PE in the outer leaflet of the plasma membrane.[12,14,17] Loss of PS and PE membrane asymmetry in *neo1-1* cells is observed even at a permissive growth temperature (27°C), but a more extensive exposure of PE occurs upon shift to a semipermissive temperature of 30°C where Neo1 is sufficiently inactivated to cause a modest growth defect.[17] Golgi glycosylation reactions are also perturbed in *neo1-ts* cells giving rise to defects in the cell wall.[12] Perhaps as a consequence of the cell wall defects, *neo1-1* cells grown at permissive temperature are larger and more elongated than normal.[12] Inactivation of *neo1-1* also causes a V-ATPase-dependent hyperacidification of vacuoles by nearly 1 pH unit, and the vacuoles in *neo1-1* cells are fragmented.[12,18] This latter phenotype implicates Neo1 in the process of vacuole membrane fusion.

Yeast vacuoles are a large organelle typically present in one to 3 copies per cell, but constantly undergo fission and fusion reactions to maintain this steady state copy number.[19] Vacuole fusion is a SNARE-dependent process regulated by the Rab protein Ypt7 and the HOPS tethering complex.[20] Ypt7 specifically recruits the multisubunit HOPS complex to the vacuole leading to close apposition of adjacent vacuole membranes along a boundary called the vertex ring.[21] Ypt7:GTP bound to HOPS then promotes the formation of a *trans*-SNARE complex that ultimately drives membrane fusion of the 2 bilayers.[20,22,23] A specific set of lipids also play a crucial role in vacuole membrane fusion *in vivo*, with isolated vacuoles *in vitro* and in reconstituted liposome fusion assays that recapitulate the role of all of the major protein complexes acting in vacuole fusion.[22,24] Ergosterol, diacylglycerol (DAG), phosphatidic acid (PA), phosphoinositides and PE have all been implicated in the vacuole membrane fusion reaction.[22,24,25] Strains deficient in production of ergosterol, DAG and phosphoinositides display fragmented vacuoles.[26,27] In addition, reagents that deplete or mask these 3 lipids inhibit fusion of vacuoles *in vitro* and these lipids are concentrated at the site of membrane fusion, the vertex ring, along with the fusion proteins.[26,28] The vacuole lipids stimulate a proteoliposome fusion assay that reconstitutes SNARE-, Ypt7- and HOPS-dependent membrane fusion, with phosphatidylcholine (PC), PI3P, PA and PE representing the minimal set of required lipids.[22,24] PE has a major influence on the proteoliposome fusion assay,[24] but unlike most of the other lipids that facilitate fusion, a role for PE had not emerged from *in vivo* studies of vacuole fusion. The data presented herein indicates that PE in the cytosolic leaflet of the membrane is an important regulator of the SNARE-mediated vacuole fusion reaction in living cells.

Results

Neo1 is a membrane protein with 10 membrane-spanning segments (Fig. 1A, gray segments), cytosolic N- and C- termini, and large cytosolic loops involved in ATP hydrolysis (Fig. 1A, white segments). Six *neo1* ts alleles (*neo1-1* to *neo1-6*) were produced by error-prone PCR for functional studies and each allele bears 6 to 16 mutations.[12] The relative positions of *neo1-1* and *neo1-2* mutations, which are non-overlapping, are shown in Fig. 1A. We had previously screened for multi-copy (2 μ) suppressors of *neo1-1* as an approach to identify processes linked to Neo1 function.[18] This screen identified several genes encoding subunits of the V-ATPase responsible for acidifying the lumen of vacuoles, endosomes and Golgi compartments. Overexpression of a single subunit perturbs assembly of the V-ATPase complex, thus attenuating V-ATPase activity.[29] The results of the suppressor screen led to the discovery that *neo1-1* mutants hyperacidify internal organelles and this partially contributes to the growth defects of *neo1-1* at nonpermissive temperatures.[18] However, we noticed that *neo1-2* was not suppressed by overexpression of *VMA11* (encoding the V-ATPase c' subunit) nearly as well as *neo1-1*. Growth of *neo1-2* at the semi-permissive temperature of 34°C was marginally improved by *VMA11* overexpression (compare 2μ *VMA11* to the empty vector control for *neo1-2* colony size), whereas *neo1-1* growth was significantly improved (Fig. 1). The allele-specific suppression of *neo1-1* by *VMA11* suggested that a screen for multicopy suppressors of *neo1-2* would recover a different set of suppressors.

YPT7 overexpression suppresses neo1-2

The *neo1-2* strain was transformed with a multicopy genomic library and a clone was isolated that partially suppressed the *neo1-2* growth defect at 37°C (Fig. 2A, 2μ clone). This genomic library clone carried a fragment of chromosome XIII containing several genes. Each gene was subcloned and tested for suppression of *neo1-2* and only *YPT7* was capable of conferring suppression (Fig. 2A, 2μ *YPT7* and unpublished observations). Surprisingly, even a single extra copy of *YPT7* carried on a centromere-based plasmid suppressed the *neo1-2* growth defect at 37°C (Fig. 2A, cen *YPT7*). In contrast, *YPT7* failed to suppress the *neo1-1* growth defect at 37°C or at a semipermissive

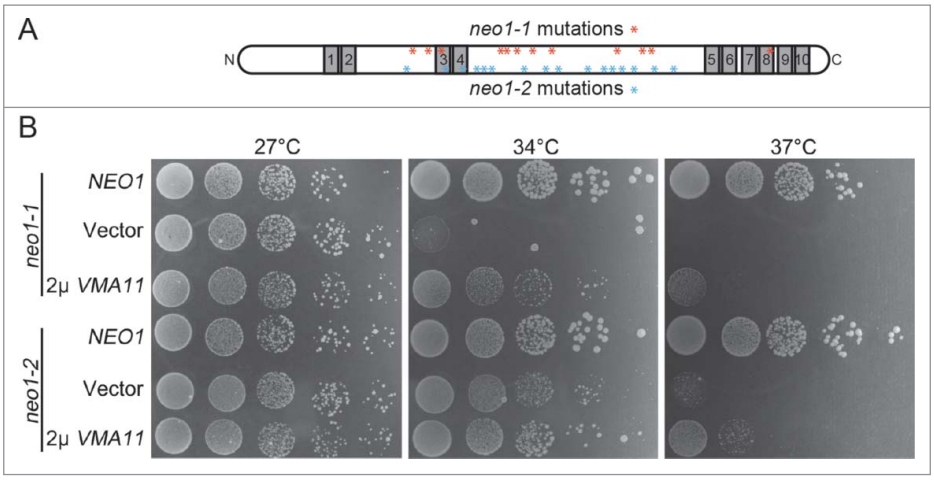

Figure 1. *VMA11* differentially suppresses the *neo1-1* and *neo1-2* growth defects at semi- or non-permissive temperatures. (A) Schematic of Neo1 showing the placement of the 10 transmembrane segments (gray). The N-terminus, C-terminus and large loops between TM2 and 3, and TM4 and 5 are cytosolic. The relative positions of the *neo1-1* and *neo1-2* mutations are indicated with asterisks (see reference 12 for the specific amino acid substitutions). *neo1 ts* mutants (YWY160, 161) harboring single copy *NEO1 (*pRS315-*NEO1)*, empty vector (pRS315) or multi-copy *VMA11* (pRS425-*VMA11*) were spotted on SD-Leu plates with serial dilution and incubated at the indicated temperatures for 3–5 d.

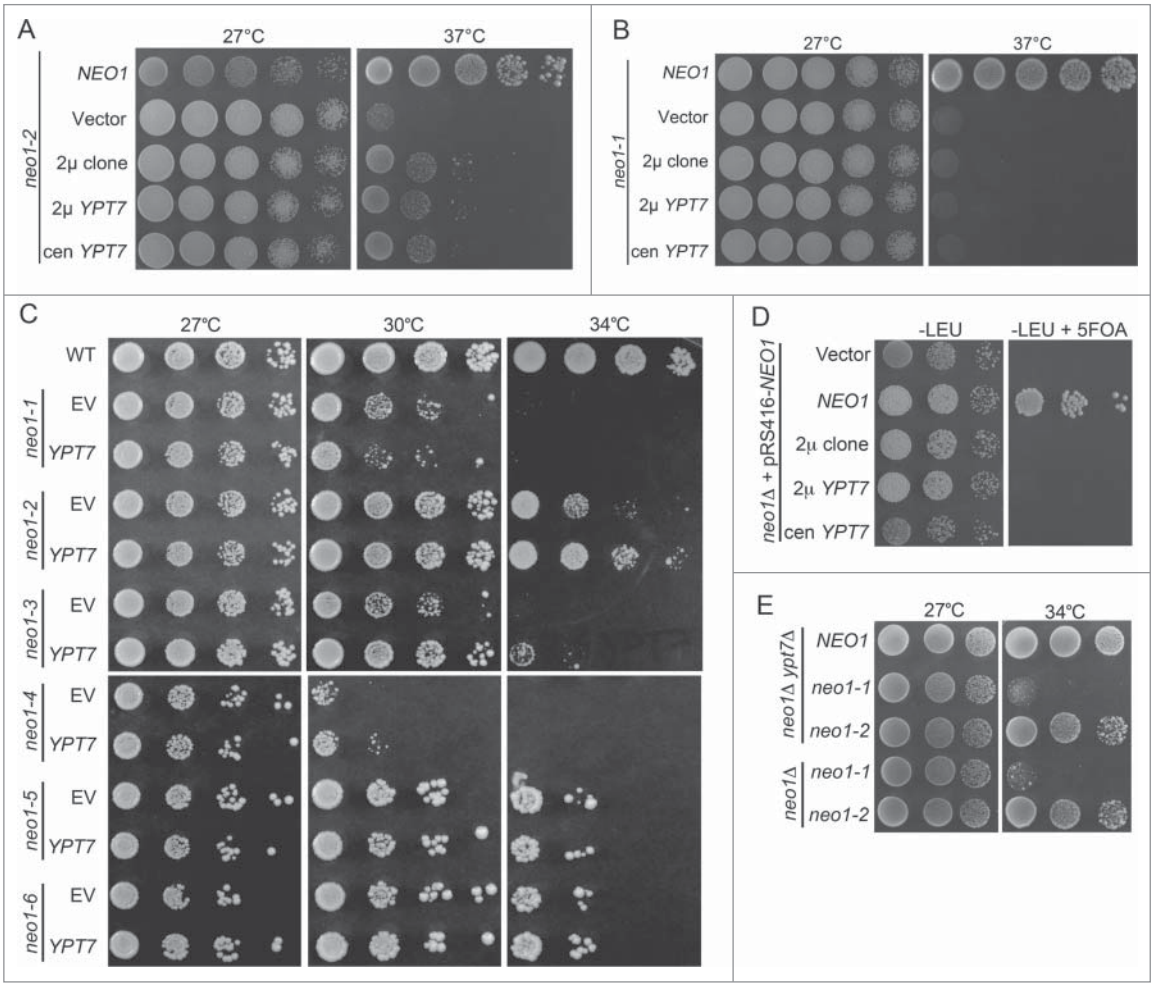

Figure 2. *YPT7* suppresses the growth defect of a subset of *neo1*^{ts} mutants. (A) *neo1-2* (YWY161) was transformed with single copy *NEO1* (YWY163), empty vector (YWY144), the multicopy genomic DNA suppressor (2 μ clone, YWY157), multicopy (2 μ) *YPT7* (YWY158) or single copy (cen) *YPT7* (YWY168) respectively. Cells were spotted on SD-Leu plates with serial dilution and incubated at indicated temperatures. (B) A *neo1-1* mutant (YWY160) was transformed with the same plasmids and tested as in (A). (C) A *neo1*Δ pRS416-*NEO1* strain (YWY10) was transformed with the same set of constructs and spotted on both SD-Leu and SD-Leu + 5FOA plates at 30°C. (D) The full collection of *neo1*^{ts} mutants (YWY148-155) carrying either empty vector or single copy *YPT7* were spotted on SD-Leu plates at permissive (27°C) or semi-permissive temperatures (30°C, 34°C) to test for suppression. (E) Plasmid shuffling assay with a *neo1*Δ strain (YWY10) to exchange pRS416-*NEO1* for an empty *LEU2*-marked plasmid (vector), or this *LEU2* plasmids carrying carrying *NEO1* or *YPT7*. The medium containing 5-FOA counter-selects the *URA3*-marked plasmid and only cells that carry complementing or suppressing *LEU2* plasmids will grow. (E) Growth of *neo1*Δ*ypt7*Δ double mutants carrying *NEO1, neo1-1* or *neo1-2* plasmids (YWY129,133,134) was compared to *neo1*Δ single mutants with *neo1-1* and *neo1-2 ts* alleles on plasmids (YWY160,161).

temperature of 30°C (Fig. 2B and C). To further test the allele specificity of suppression, *YPT7* or an empty vector was used to transform all 6 independently isolated *neo1* ts mutants (*neo1-1* – *neo1-6*,[12]). Of this group, a single extra copy of *YPT7* partially suppressed *neo1-2, neo1-3* and *neo1-4*, but no suppression was observed for *neo1-5* and *neo1-6* (Fig. 2C). While many of the mutations cluster near each other in the large cytosolic domains, there are no common mutations between *neo1-2, neo1-3* and *neo1-4* that could provide a simple explanation for the allele-specific suppression by *YPT7*.[12]

To test if *YPT7* could suppress the lethality caused by deletion of *NEO1*, we generated haploid *neo1Δ* strains covered by *NEO1* on a *URA3*-marked plasmid and harboring the same set of *YPT7* clones on *LEU2*-marked plasmids. These strains were serially diluted onto medium containing 5-fluoro-orotic acid (5-FOA) to select for cells capable of losing the *NEO1-URA3* plasmid. Only the strain carrying a wild-type *NEO1-LEU2* control plasmid was able to grow on 5-FOA, while the strains carrying an empty *LEU2* vector or the indicated *YPT7* clones failed to grow (Fig. 2D). This result indicates that *YPT7* cannot bypass the essential function of *NEO1*. We then asked if removing *YPT7* would have the opposite effect and exacerbate *neo1-2* growth defects. For this experiment, we used *neo1Δ* and *neo1Δ ypt7Δ* strains expressing *NEO1, neo1-1* or *neo1-2* from plasmids. However, no difference in growth was observed for *neo1-1* or *neo1-2* in the presence or absence of *YPT7* (Fig. 2E).

Neo1 localization to Golgi and endosomes

The allele-specific suppression of *neo1-2* by *YPT7* could suggest a direct interaction between the encoded proteins. However, Ypt7 localizes to the vacuole where it regulates membrane fusion reactions and Neo1 has not been reported to localize to the vacuole.[12-14,30] However, Neo1 is weakly expressed and localization experiments with functional, epitope- or GFP-tagged forms of Neo1 expressed at endogenous levels reported a broad localization in the ER, Golgi and endosomes, but may have missed a minor fraction of Neo1 in the vacuole membrane. Therefore, we tested if overexpression of a functional, GFP-tagged Neo1 would allow us to detect any Neo1 in the vacuole membrane. GFP-Neo1 (N-terminally tagged) expressed from the moderate-strength alcohol dehydrogenase (*ADH*) promoter[31] co-localized partially with markers of the early Golgi (COP1-mKate), medial Golgi (Aur1-mKate) and late Golgi (Sec7-mKate)(Fig. 3A–C).[32] The Pearson's correlation coefficient (r) was slightly higher for the GFP-Neo1 and Aur1-mKate pair perhaps indicating preferential localization of GFP-Neo1 to the medial Golgi at this level of expression.

GFP-Neo1 was also detected in late endosomes marked with DsRed-FYVE (Fig. 3D),[33] although only 33% of the cells showed co-localization of GFP-Neo1 with the late endosome marker while every cell showed co-localization with the Golgi markers. A C-terminally epitope tagged form of Neo1 was previously detected in the ER and Golgi,[12] but GFP-Neo1 was not detected in the ER even though it was more highly expressed. Importantly, GFP-Neo1 was not detected in the vacuole membrane (marked with a "v" in a few of the cells in Fig. 3) at the moderate expression level driven by the *ADH* promoter. To drive very high expression, we placed *GFP-NEO1* under control of the strong glycerol 3-phosphate dehydrogenase (*GPD*) promoter[31] and expressed the construct from a multicopy plasmid. With these conditions, we can detect vacuole membrane localization of GFP-Neo1 (Fig. 3E, compare the rings of GFP-Neo1 fluorescence to the vacuoles in the DIC image that appear as large depressions in the cells). GFP-Neo1 also localized strongly to a structure adjacent to the vacuoles (arrowheads), which are likely prevacuolar endosomes. Thus, we can only detect GFP-Neo1 in the vacuole membrane when it is expressed at very high, nonphysiological levels.

The observation that GFP-Neo1 mislocalized to the vacuole membrane when highly overexpressed suggested that a saturable retention or retrieval mechanism was acting to maintain a steady-state localization in the Golgi. Because GFP-Neo1 appears to traffic into the late endosome, we tested if retromer was involved in the localization of Neo1. GFP-Neo1 expressed from the *ADH* promoter was readily detected in the vacuole membrane of *vps35Δ* cells that are deficient for a retromer subunit (Fig. 4A). In contrast, 2 related P4-ATPases, GFP-Drs2 and GFP-Dnf1,[34] were not mislocalized to the vacuole in *vps35Δ* cells, suggesting that they do not traffic into the late endosome (Fig. 4B). These data suggest that Neo1 is a cargo of retromer and is retrieved from the late endosome to the Golgi to prevent missorting to the vacuole.

YPT7 suppresses the fragmented vacuole phenotype of neo1-2

We next examined vacuole morphology in *neo1-ts* cells and asked if *YPT7* overexpression could suppress the fragmented vacuole phenotype of these mutants. WT, *neo1-1* and *neo1-2* cells expressing *YPT7* or an empty vector were grown at the permissive temperature of 30°C and stained with FM4-64 to visualize vacuoles. The WT cells exhibited an average of 2.4 vacuoles per cell while the *neo1-1* and *neo1-2* exhibited 3.25 and 3.6 vacuoles per cell, respectively (Fig. 5). *YPT7* expressed from single-copy (cen) or multicopy (2 μ) vectors suppressed the fragmented vacuole phenotype to WT values in *neo1-2* cells (Fig. 5A and B), but not *neo1-1* cells (Fig. 5C and D). Therefore, the defect in vacuole fusion caused by *neo1-2* can be overcome by modest overexpression of *YPT7*.

Disruption of *YPT7* causes highly fragmented vacuoles[30] and it is possible that *neo1* mutants expressed lower amounts of Ypt7 relative to WT cells, which led to vacuole fragmentation. However, quantitative western blotting showed no significant difference in Ypt7 levels between WT, *neo1-1* and *neo1-2* strains (Fig. 5E and F). Cells carrying an additional copy of *YPT7* on centromere-based plasmids expressed 3-fold more Ypt7 than WT cells, providing an explanation for the dosage suppression by the low copy plasmids. The slightly higher expression of Ypt7 from the plasmids in *neo1-2* relative to *neo1-1* (compare lane 4 to lane 6) is unlikely to be the cause of the allele-specific suppression because even higher Ypt7 expression from a multicopy plasmid failed to suppress *neo1-1* growth defects (Fig. 2).

It is also possible that *YPT7* overexpression may somehow protect the mutant Neo1-2 protein from thermal inactivation, thereby conferring suppression. If this is the case, then all

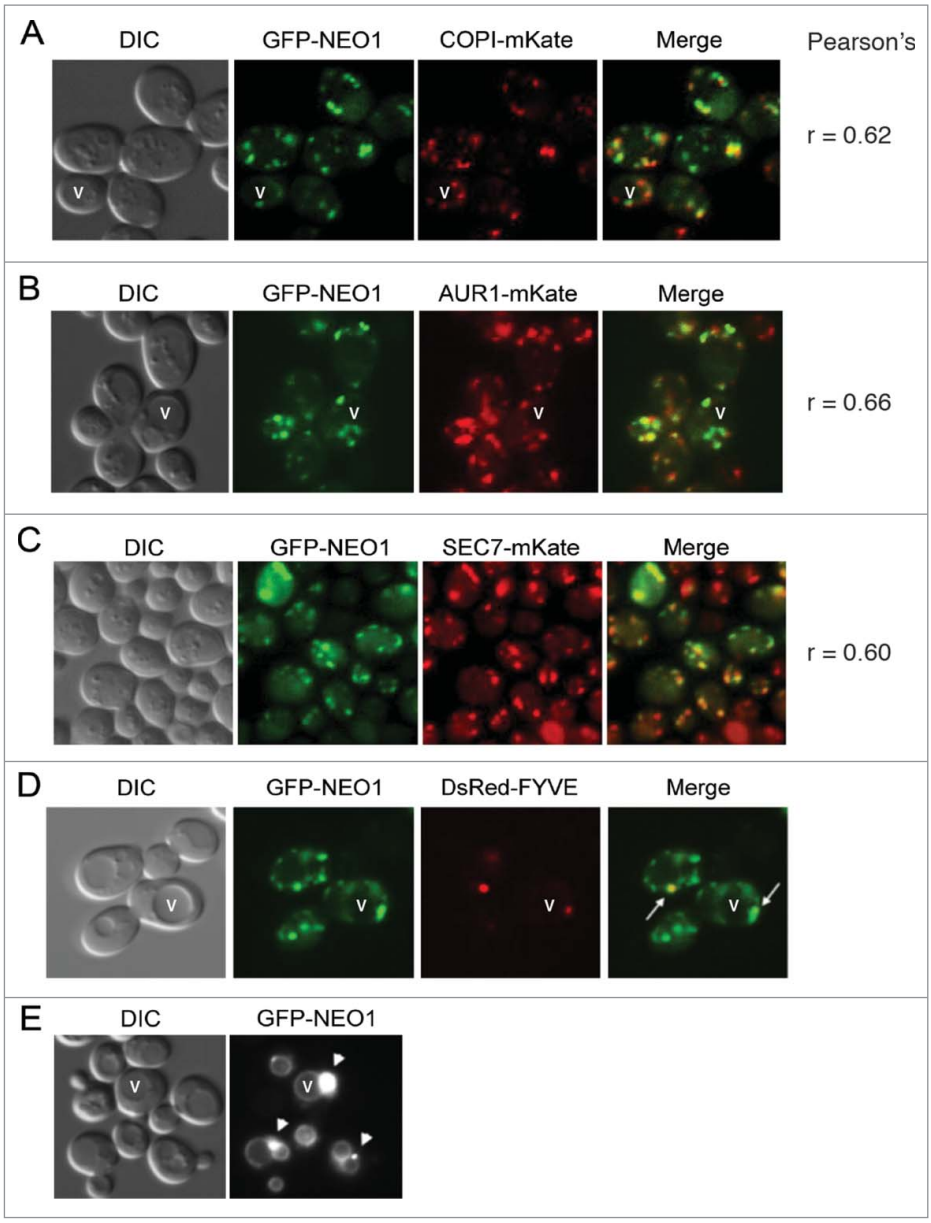

Figure 3. Localization of GFP tagged Neo1p at different levels of expression. (A-C) The construct pRS313-P_{Adh}-*GFP-NEO1* was transformed into strains harboring different Golgi markers genomically tagged with mKate in the BY4742 background (YWY208-210) and imaged. The Pearson's correlation coefficient (r) was determined using imageJ's co-localization function. (D) A *neo1Δ* strain harboring pRS313-P_{Adh}-*GFP-NEO1* (which functionally complements *neo1Δ* to support growth) and pRS425-DsRED-FYVE (late endosomal marker)(YWY128) was imaged. Arrows indicate the overlap between GFP-Neo1 decorated puncta and DsRED-FYVE decorated late endosomes. (E) GFP-NEO1 was highly overexpressed from the GPD promoter in *neo1Δ* cells (YWY172) and imaged. All strains were cultured overnight and sub-cultured the next morning at 30°C. Cells were harvested at A_{600} ~0.6 and imaged.

phenotypes exhibited by *neo1-2* should be suppressed. Inactivation of Neo1 leads to a defect in the COPI-dependent transport of Rer1-GFP from the Golgi to the ER and mislocalization of this reporter to the vacuole.[12,35] We examined Rer1-GFP trafficking in *neo1-2* cells with or without *YPT7* and could not detect any suppression of the Rer1-GFP trafficking defect (Fig. 6). For these data, we found cells in the population with primarily one large vacuole to display to avoid the confounding affect of vacuole morphological changes.

PE deficiency cause vacuole fragmentation

Inactivation of Neo1 causes a loss of plasma membrane asymmetry for both PS and PE, although the interleaflet distribution of PE is more strongly affected than PS.[17] PE has also been implicated in membrane fusion reactions driven by the vacuolar SNARE proteins.[24] Therefore, it seemed likely that the fragmented vacuole phenotype in *neo1-ts* cells was caused by perturbation of PE distribution. If so, then other means of reducing PE in the vacuole membrane should also lead to fragmented vacuoles. PE is an essential lipid in budding yeast and is synthesized primarily by decarboxylation of PS and by the Kennedy salvage pathway using ethanolamine as a precursor (Fig. 7A).[36] To determine if PE deficiency in vivo influences vacuolar morphology, we stained cells deficient for the PS decarboxylases (*psd1Δ*, *psd2Δ* and *psd1Δ psd2Δ*) with FM4-64. As predicted, deletion of *PSD1*, encoding the mitochondrial PS decarboxylase that synthesizes more than half of the total

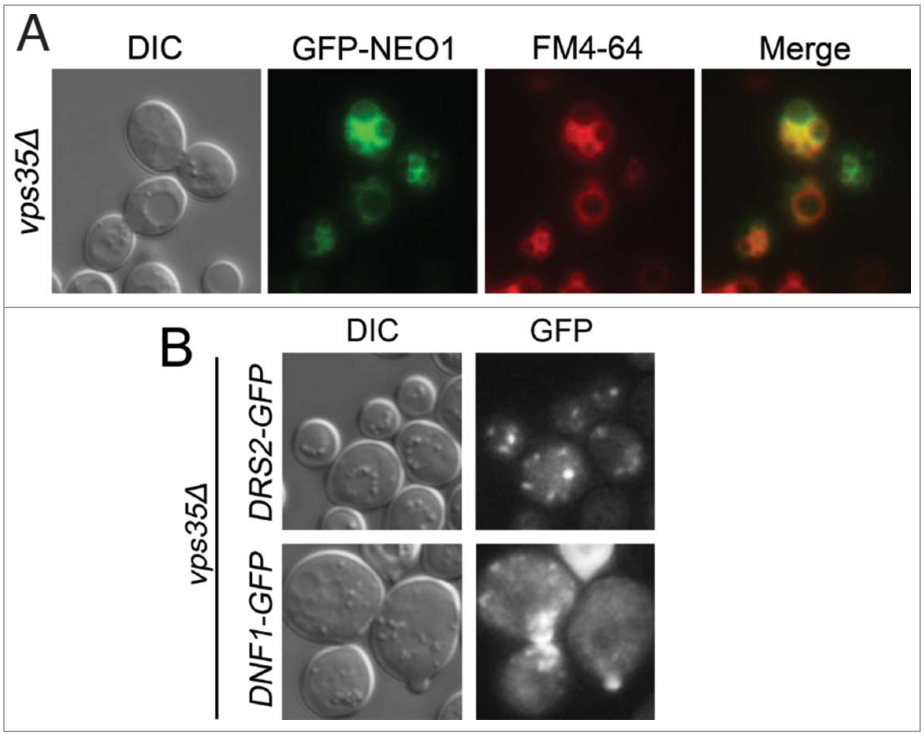

Figure 4. Trafficking of Neo1p is controlled by the retromer complex. (A) A *vps35*Δ (retromer) mutant expressing pRS413-P_{Adh}-*GFP-NEO1* (YWY173) was stained with 32 μM FM4-64 for 20 minutes followed by 1 hour incubation in YPD at 30°C. Cells were rinsed twice with imaging buffer (PBS + 2% glucose) before imaging. (B) Images of a *vps35*Δ mutant expressing pRS416-P_{CPY}-*DRS2-GFP* together with pRS425-*CDC50* (top, YWY174) or pRS416-P_{CPY}-*DNF1-GFP* together with pRS425-*LEM3* (YWY175).

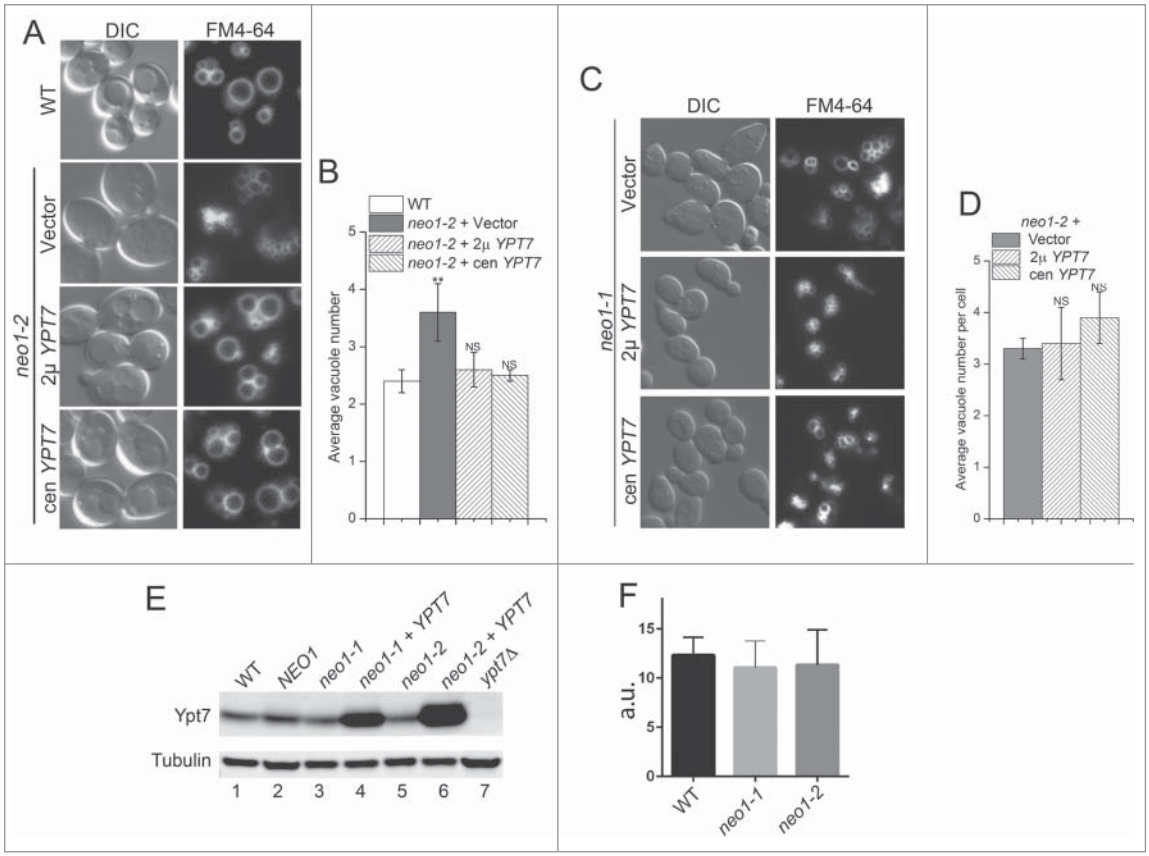

Figure 5. *YPT7* suppresses the fragmented vacuole phenotype of a *neo1-2* mutant. (A and C) The WT (BY4741), *neo1-2* (YWY161), and *neo1-1* (YWY160) strains indicated were stained with FM4-64 to mark vacuoles and imaged. (B and D) The average vacuole number per cell was quantified from single image planes of approximately 100 cells, and the average of 3 separate experiments +/− s.e.m.. A student t test was used to compare *neo1-ts* cells expressing different constructs with WT cells (**, $p < 0.01$;NS, not significant). (E) An equal number of cells from the indicated strains were lysed in SDS sample buffer and subject to immunoblotting with anti-Ypt7 and anti-tubulin. Ypt7 was overexpressed in *neo1-1* and *neo1-2* strains from single-copy, centromeric plasmids. (F) Quantitation of Ypt7 band intensities from 3 immunoblots (+/− s.e.m.; a.u., arbitrary units).

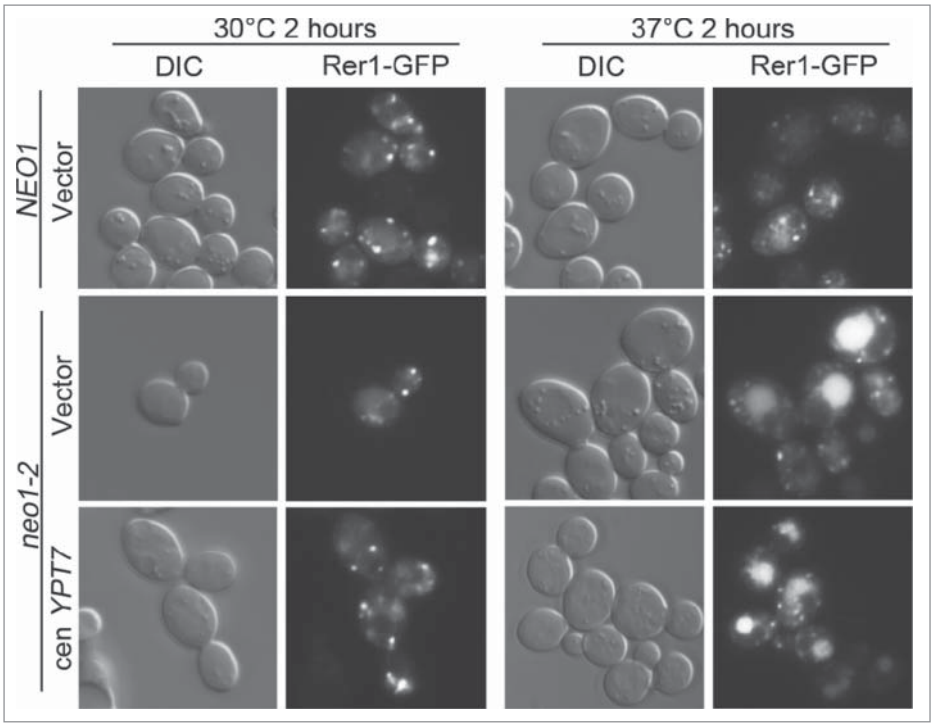

Figure 6. *YPT7* does not suppress the *neo1-2* Rer1-GFP protein transport defect. *neo1-2* strains expressing Rer1-GFP and harboring an empty vector or single copy *YPT7* (YWY177-178) was cultured overnight and sub-cultured the next morning at 27°C. After reaching log growth phase, an equal amount of cells were shifted to 30°C or 37°C for 2 hours. A *neo1*Δ pRS313-*NEO1* strain (YWY176) expressing Rer1-GFP was imaged as a control.

cellular PE,[36] resulted in significantly fragmented vacuoles as compared to WT cells. Deletion of *PSD2*, encoding a Golgi/endosomal PS decarboxylase with a minor contribution to total PE content (~5%),[36,37] resulted in no significant difference in vacuole number compared to WT cells (Fig. 7B and C). Deletion of *PSD1* and *PSD2* resulted in highly fragmented vacuoles with ~90% of the cells displaying 5 or more vacuoles (Fig. 7D and E).

PE can be further processed through methylation to PC and so *psd1Δ psd2Δ* diminishes both PE and PC levels in the cells.

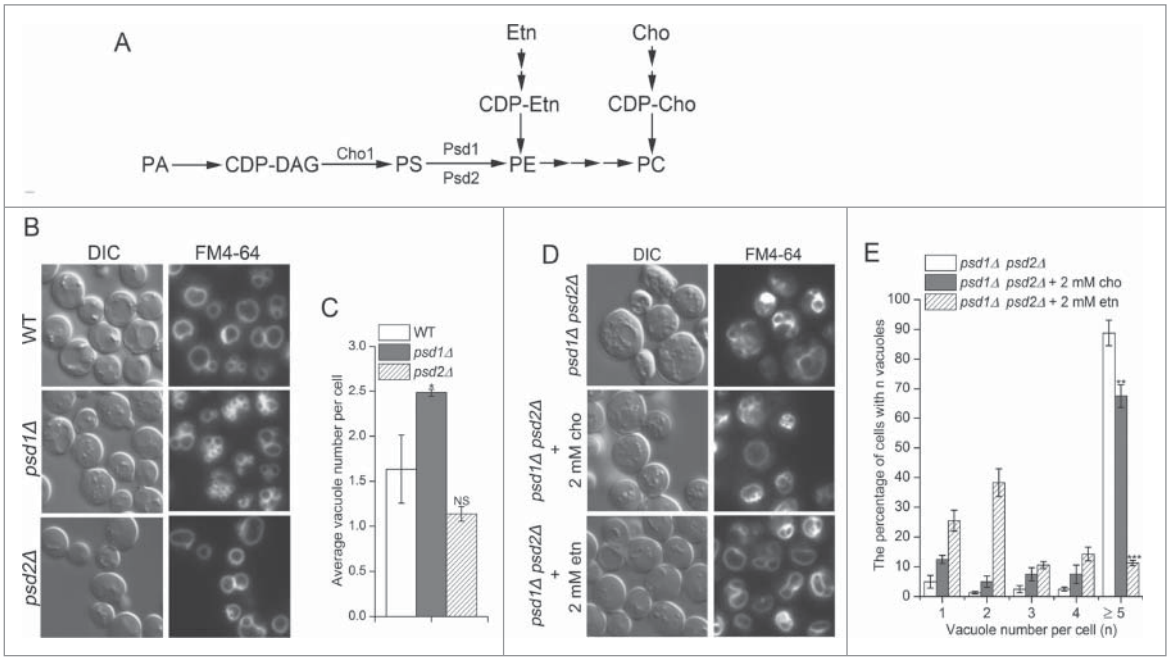

Figure 7. PE is crucial for vacuole fusion *in vivo*. (A) Pathways for synthesis of PS, PE and PC in *Saccharomyces cerevisiae*. WT (SEY6210), *psd1*Δ and *psd2*Δ cells (KGS20,21) were stained with FM4-64 to visualize vacuole morphology. (B) Average number of vacuoles per cell was quantified for cells from (A). *, $p < 0.05$, NS, non-significant. (C) The *psd1*Δ*psd2*Δ double mutant (KGS22) was supplemented with 2 mM choline (cho) or 2 mM ethanolamine (etn) and stained with FM4-64. The number of vacuoles per cell (single image plane) was plotted as a percentage of cells in each category. The percentage of cells with 5 or more vacuoles was compared with *psd1*Δ*psd2*Δ cells without choline or ethanolamine supplement using Student's t test. **, $p < 0.01$, ***, $p < 0.001$.

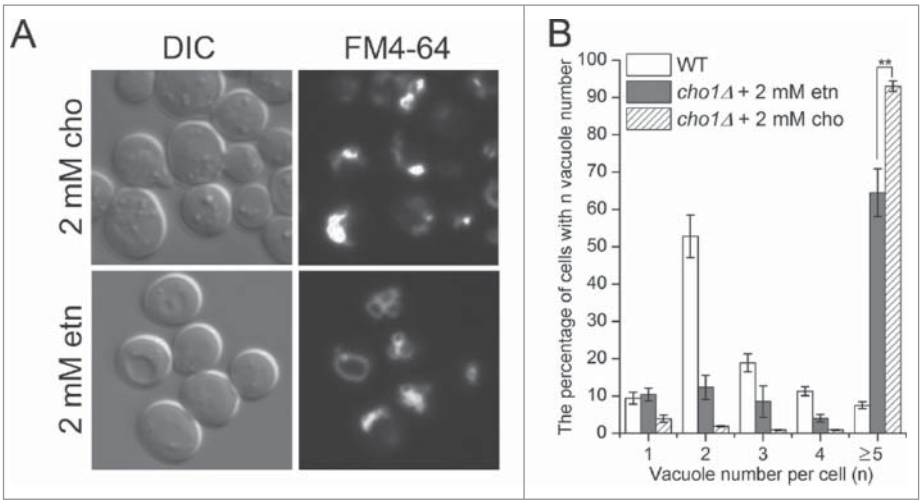

Figure 8. Ethanolamine supplementation reduces vacuole fragmentation in *cho1Δ* cells. (A) *cho1*Δ cells (RBY8700) were cultured with 2 mM choline or 2 mM ethanolamine and stained with FM4-64. *cho1*Δ is inviable in synthetic media without supplement of choline or ethanolamine. (B) The number of vacuoles per cell (single image plane) was plotted as a percentage of cells in each category. **, $p < 0.01$.

To distinguish whether a reduction in PE or PC, or an increase in PS, caused vacuole fragmentation in *psd1Δ psd2Δ* cells, we tested if supplementation of cells with choline (cho) or ethanolamine (etn) to increase flux through the salvage pathways could suppress this phenotype. Choline supplementation modestly decreased the number of vacuoles per *psd1Δ psd2Δ* cell. In contrast, ethanolamine supplementation to stimulate PE synthesis dramatically decreased vacuole number (Fig. 7D and E). Thus, reduced PE content of the cells rather than reduced PC or increased PS caused the vacuole fragmentation.

Deletion of the PS synthase gene (*CHO1*) eliminates PS and reduces flux to PE and PC through the de novo synthesis pathway (Fig. 7A). Growth of *cho1Δ* cells requires supplementation with either choline or ethanolamine and cells grown on choline to support PC synthesis have highly fragmented vacuoles (Fig. 8A and B), comparable to *psd1Δ psd2Δ* cells. Again, ethanolamine supplementation to increase PE synthesis through the salvage pathway significantly reduced vacuole number in *cho1Δ* cells, although not as effectively as observed for *psd1Δ psd2Δ* cells. Together, these data indicate that PE is a crucial membrane lipid for vacuole fusion events *in vivo*, even in the absence of PS.

Deletion of *PSD1* alone produces a fragmented vacuole phenotype that is similar to *neo1-2*. Therefore, we tested if overexpression of *YPT7* could suppress the fragmented vacuole phenotype of *psd1Δ* cells. Surprisingly, we found no significant difference in average vacuole number between *psd1Δ* cells with or without additional copies of *YPT7* (Fig. 9). We also tested if ethanolamine supplementation could suppress the *neo1-2* vacuole fragmentation phenotype, but surprisingly found no significant suppression (Fig. 10A and B). However, modest overexpression of *PSD2* (carried on a single-copy plasmid and expressed from the ADH promoter) was able to significantly suppress the fragmented vacuole phenotype of *neo1-2* (Fig. 10A and B), although growth of *neo1-2* at 37°C was only marginally improved by *PSD2* overexpression (Fig. 10C). These data are consistent with PE being a key lipid in vacuole fusion.

In addition to its role in vacuolar fusion, Ypt7 recruits Vps39 to the vacuole membrane to facilitate formation of a membrane contact site between the vacuole and mitochondria called vCLAMP (*v*acuol*e* and *m*itochondria *p*atch), a structure that may allow transfer of PE from the mitochondria to the vacuole membrane. Thus, it was possible that *YPT7* overexpression suppressed vacuole fragmentation in *neo1-2* cells by enhancing the formation of vCLAMP. In this case, we would also expect *VPS39* overexpression to suppress *neo1-2*. However, *VPS39* overexpression failed to suppress *neo1-2* growth defects. V*PS39* also failed to enhance *neo1-2* suppression when co-expressed with *YPT7* (Fig. 11). Thus, it is unlikely that Ypt7 suppresses *neo1-2* by enhancing formation of vCLAMP.

Discussion

PE has been implicated in vacuole membrane fusion based on in vitro liposome-based assays that reconstitutes SNARE-dependent fusion.[24] Here we report that PE also plays a crucial role in vacuole membrane fusion *in vivo*. Deletion of *PSD1*, encoding a mitochondrial PS decarboxylase responsible for synthesis of ~50% of the vacuolar PE,[37] causes vacuole fragmentation. Even though Psd2 localizes to endosomal membranes, it only makes a modest contribution (~5%) to vacuole PE levels[37] and the *psd2Δ* mutant does not display fragmented vacuoles. Deletion of both *PSD1* and *PSD2* causes severe vacuole fragmentation, but supplementing these cells with ethanolamine to stimulate PE synthesis through the Kennedy pathway markedly suppresses the fragmentation phenotype (Fig. 7). Neo1 mutants also cause fragmented vacuoles and a loss of PS and PE asymmetry. The observation that Psd2 overexpression (which should enhance PE levels at the expense of PS) suppresses the vacuole fragmentation in *neo1-2* strongly suggests it is a perturbation of PE in the vacuole membrane that initially causes the fragmented vacuole phenotype. These results demonstrate an important role for PE in vacuole fusion and imply that inactivation of Neo1 perturbs PE availability to the fusion machinery in the vacuole membrane.

Budding yeast strains harboring a disruption of *NEO1* are inviable in spite of the presence of 4 additional P4-ATPases (Drs2, Dnf1, Dnf2 and Dnf3) that traffic through the Golgi and

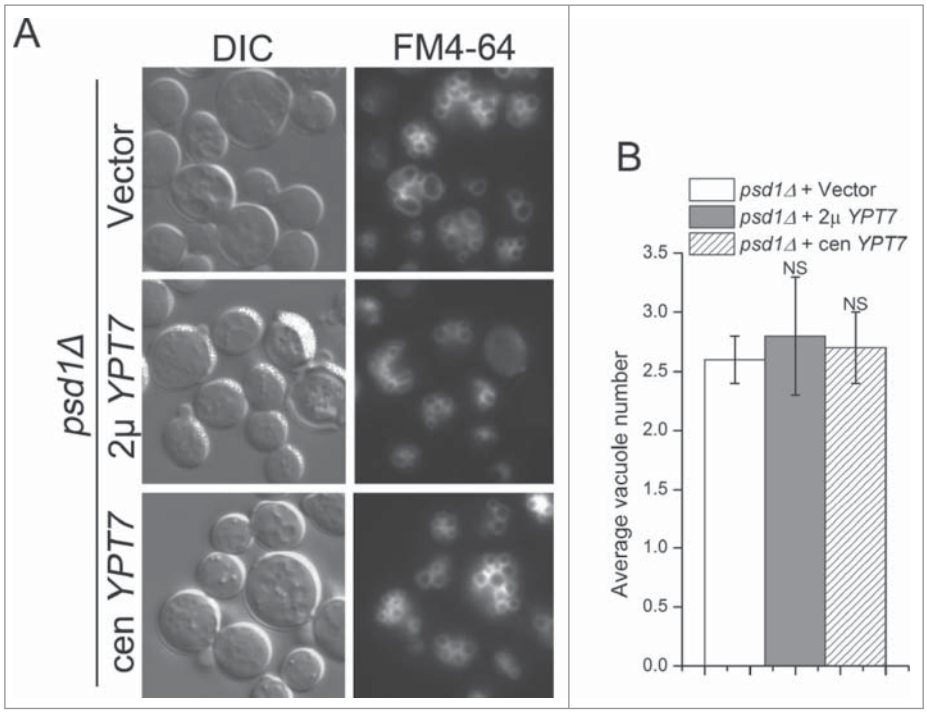

Figure 9. *YPT7* does not suppress the fragmented vacuole phenotype of *psd1*Δ. (A) *psd1*Δ cells harboring an empty vector, multicopy (2 μ) *YPT7* or single copy (cen) *YPT7* (YWY140-142) were stained with FM4-64 to visualize vacuole morphology. (B) The average vacuole number of the cells from (A) was quantified. NS, not significant.

endosomal system where Neo1 resides. Among the budding yeast P4-ATPases, *neo1* mutations uniquely cause vacuole fragmentation and deletion of other P4-ATPases genes, alone or in combination, does not lead to a comparable fragmented vacuolar phenotype.[11] Interestingly, both *dnf1Δ dnf2Δ* and *neo1-ts* mutants substantially hyperacidify vacuoles, yet the *dnf1Δ dnf2Δ* cells have 1 – 3 large vacuoles per cell, as do WT cells.[18] These observations suggest that Neo1 has a unique substrate that is specifically required for vacuole fusion, most likely PE, but shares a substrate with Dnf1 and Dnf2 that influences vacuolar

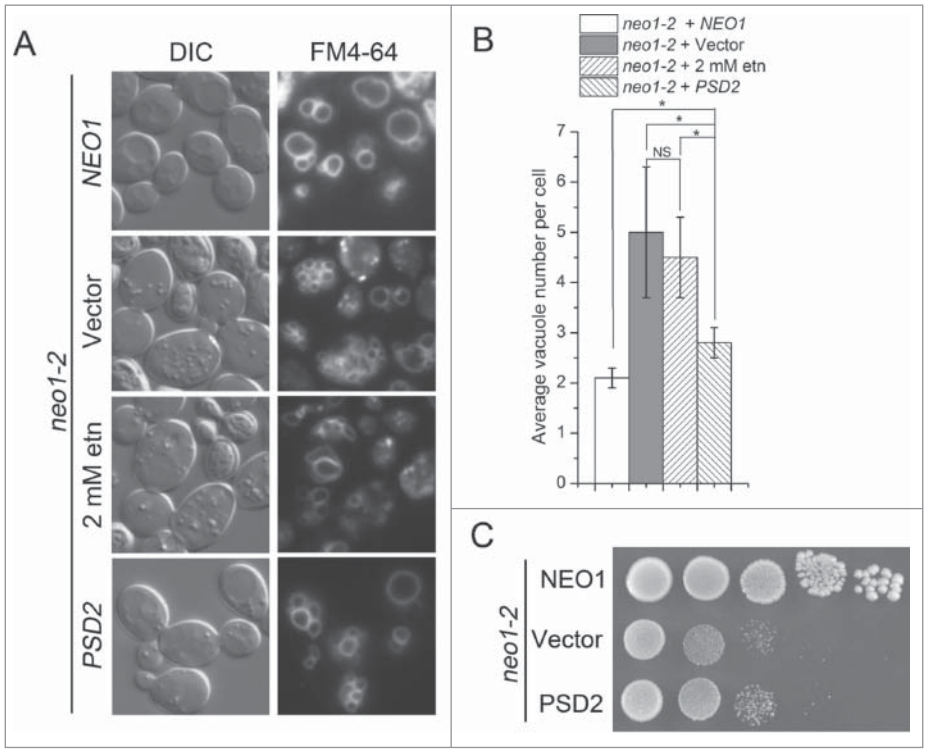

Figure 10. Ethanolamine supplementation and *PSD2* partially suppresses the fragmented vacuole phenotype of *neo1-2* cells. (A) *neo1-2* cells transformed with *NEO1*, empty vector or *PSD2* (YWY179-181), or supplemented with 2 mM ethanolamine during growth at 30°C, were stained with FM4-64. (B) The average vacuole number per cell in strains from (A) was quantified. *, $p < 0.05$, NS, not significant. (C) Strains from (A) were spotted on SD-Ura plates and incubated at 37°C for 4 d.

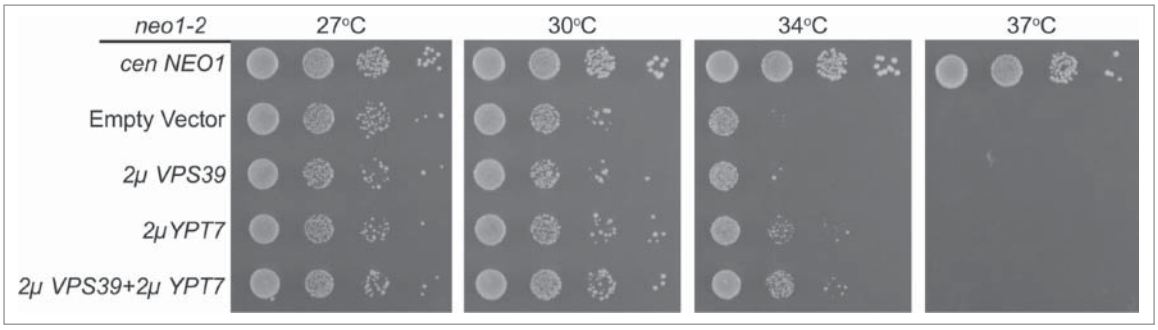

Figure 11. Overexpression of *VPS39* fails to suppress *neo1-2* growth defects. *neo1-2* strains (from top to bottom: MTY10-39, MTY144-39, MTY158-39 and MTY200-39) expressing the indicated multicopy constructs were grown with serial dilution at the temperatures indicated.

pH. While Dnf1 and Dnf2 translocate fluorescent derivatives of PE efficiently, these P4-ATPases may preferentially transport lysoPE bearing a single fatty acyl chain and perhaps it is loss of lysoPE asymmetry that influences vacuolar pH.[1] Dnf3 is reported to flip PE,[38] but this protein is very weakly expressed in budding yeast grown in standard laboratory conditions.[11] Drs2 is the major PS flippase in yeast and may also have a weak activity toward PE,[39] but Drs2 clearly cannot compensate for the loss of Neo1.[17] We speculate that Neo1 is the primary flippase for dually acylated PE in yeast and is needed to concentrate PE on the cytosolic leaflet of Golgi and late endosomes.

None of the P4-ATPases, including Neo1, localize to the vacuole membrane when expressed at endogenous levels or when modestly overexpressed.[11,12,14,40,41] Neo1 primarily localizes to the Golgi and we could only detect GFP-Neo1 in the vacuole membrane when expressed from a very strong GPD promoter on a multicopy plasmid, which should generate more than 100-fold more Neo1 than WT cells.[31] Mutation of a retromer component involved in late endosome to Golgi retrieval of proteins also led to vacuolar localization at more modest levels of Neo1 expression. Therefore, it seems unlikely that Neo1 is functionally present in the vacuole membrane of WT cells, or that the suppression of *neo1-ts* by Ypt7 overexpression is mediated by a direct interaction between the Neo1 and the vacuolar localized Ypt7. It is more likely that PE traveling the secretory pathway toward the vacuole is concentrated in the cytosolic leaflet by Neo1 at the level of the Golgi or late endosome prior to arrival at the vacuole. Loss of Neo1 activity could therefore lead to less PE in the cytosolic leaflet of the vacuoles. It is also possible that sorting of SNAREs involved in vacuolar fusion is partially perturbed by *neo1^{ts}* mutants at the level of the endosomes or Golgi, thereby reducing their concentration in the vacuolar membrane leading to reduced fusion. In this case, increasing Ypt7 or PE concentration on the vacuole may restore wild-type kinetics of fusion with fewer SNAREs.

The observation that only certain *neo1^{ts}* alleles (*neo1-2*, *neo1-3*, and *neo1-4*) can be suppressed by Ypt7 overexpression may reflect the degree to which PE concentration in the vacuolar membrane cytosolic leaflet is perturbed by the *neo1^{ts}* mutant. Ypt7 may only suppress *neo1^{ts}* mutants that reduce PE levels just below a threshold needed for efficient SNARE-mediated fusion. More severely affected mutants, such as *neo1-1*[17] or *psd1Δ*[37] may have too little PE in the membranes to support efficient fusion regardless of the Ypt7 concentration. It is also possible that the *neo1* mutations that are suppressed by *YPT7* alter substrate preference in a unique manner. For example, Neo1 might transport several different phospholipid species differing in either headgroup or acyl chain composition (length and number of double bonds) and the mutations may change these patterns of recognition. Similarly, we find that overexpression of *VMA11* suppresses *neo1-1* better than it suppresses *neo1-2*. Clearly these *neo1-1* and *neo1-2* mutations are differentially affecting Neo1 functions and defining the nature of these differences is an important goal.

The observed suppression of *neo1-2* by *YPT7* overexpression could imply that cytosolic PE influences Ypt7 activity in vacuole fusion. This could occur through a direct interaction of Ypt7 with PE, or by an influence of PE on the Ypt7 GEF (Mon1-Ccz1 heterodimer) and/or GAP (Gyp1 or Gyp7). However, the vacuolar SNARE-dependent liposome fusion assay requires PE when reconstituted with Ypt7-GTP in the absence of the Ypt7 GEF and GAP, indicating that PE has an important role in vacuole fusion downstream of Ypt7 activation.[42] The conically-shaped PE molecule is thought to produce packing defects in the monolayer that facilitate initiation of a hemifusion intermediate driven by zippering of v-SNARE and t-SNAREs in apposing membranes.[19,25] One explanation for the suppression of *neo1-2* by Ypt7 is that a concentration of PE that is suboptimal to support efficient SNARE catalyzed fusion can be overcome by increasing Ypt7-GTP and HOPS concentration on the vacuolar membrane to enhance tethering and SNARE assembly.

Further tests of the hypotheses described herein will require development of probes that can be used to measure the *trans*-bilayer distribution of PE in vacuolar membranes of living cells. Alternatively, it would be necessary to reconstitute vacuolar membrane fusion in a proteoliposome system of not only defined composition, but with also an asymmetric distribution of PE between the lumenal and cytosolic leaflet. Because of these technical limitations, we cannot definitively conclude that the fusion defect is caused by the loss of vacuole membrane PE asymmetry in *neo1^{ts}* mutants. However, we can conclude that perturbations in PE metabolism disrupt vacuole fusion *in vivo*.

Materials and methods

Media, plasmids and strains

Yeast strains were maintained in complete medium (YP, 1% yeast extract, 2% peptone) or synthetic minimal (SM) medium

supplemented with 2% glucose. Sporulation was performed by culturing cells in presporulation media (0.8% yeast extract, 0.3% peptone, 10% glucose) until saturation before shifting to sporulation media (1% KOAc, 0.1% yeast extract, 0.05% glucose) for 3-7 d at 30°C. For random sporulation analysis, sporulated cells were treated with 0.8% glusulase for 15 minutes and then vortexed with equal amount of ether for 30 seconds. The spores were then spread on selective plates.

Plasmids used in this study are listed in Table S1. A *NEO1* genomic DNA fragment with 518 bp upstream and 126 bp downstream of the *NEO1* open reading frame (ORF) was amplified from yeast genomic DNA using primers containing BamHI and XhoI restriction sites and cloned into pRS416 to generate *pRS416-NEO1*. The same *NEO1* fragment was cloned into pRS315 to generate *pRS315-NEO1*. The restriction sites used in pRS315 were BamHI and SalI, therefore both XhoI and SalI sites were destroyed when *NEO1* was inserted. The *NEO1* coding sequence was amplified from *pRS416-NEO1* using primers containing BamHI and SalI sites and cloned into pRS413-P_{NEO1}.[43] For *pRS413-P_{ADH}-GFP-NEO1, GFP* was amplified from pEGFP-C1 (clontech) using primers containing XbaI and BamHI sites and digested with indicated enzymes, *NEO1* coding sequence was removed from *pRS413-P_{NEO1}-NEO1* using BamHI and SalI, and pRS413-P_{ADH} was digested with XbaI and SalI. These three pieces were then ligated. The *GFP-NEO1* fragment was released from *pRS413-P_{ADH}-GFP-NEO1* using XbaI and SalI, and ligated into pRS423-P_{GPD} digested with SpeI and SalI. All constructs carrying GFP-tagged Neo1 fully supported growth of a *neo1Δ* strain, indicating that GFP-Neo1 is functional. A *YPT7* genomic DNA fragment with 501 bp upstream and 153 bp downstream of coding sequence was amplified from yeast genomic DNA using primers containing BamHI and SalI sites and cloned into pRS315 and pRS425 to generate *pRS315-YPT7* and *pRS425-YPT7*.

The same strategy used to generate *pRS413-P_{ADH}-GFP-NEO1* was used to generate *pRS416-P_{ADH}-GFP-YPT7*. The *GFP* fragment was amplified from pYM-N13[44] using primers containing BamHI and HindIII sites, the *YPT7* coding sequence was amplified from *pRS315-YPT7* using primers containing HindIII and XhoI sites, and pRS416-P_{ADH} was digested with BamHI and XhoI and 3 pieces were then ligated. The *PSD2* coding sequence was amplified from yeast genomic DNA using primers containing EcoRI and SalI sites. The fragment was then digested and cloned into pRS416-P_{ADH}. A genomic *VPS39* region of 3.95kb was amplified with indicated primers and ligated to BamHI-SalI linearized *pRS416* and *pRS426* to generate *pRS416-P_{VPS39}-VPS39* and *pRS426-P_{VPS39}-VPS39* plasmids. All plasmid generated were confirmed by sequencing.

Yeast strains used in this study are listed in Table S2. The plasmid *pRS416-NEO1* was transformed into *BY4743 neo1Δ* and the resulting cells were sporulated. After random sporulation, spore YWY10 (*MATa his3 leu2 met15 ura3 lys2 neo1ΔpRS416-NEO1*) was selected on SD plates with G418 but lacking uracil. A plasmid-shuffling strategy was used to replace the plasmid *pRS416-NEO1* in YWY10 with plasmids containing *neo1 ts* alleles. *pRS413-neo1-1* and *pRS413-neo1-2* was transformed into YWY10 and the resulting cells were selected with 5FOA to exclude *pRS416-NEO1*. The resulting strains were YWY160 and YWY161. Homologous recombination was used for disrupting *YPT7* in YWY10. About 50-60 bp flanking homologous sequences immediately outside *YPT7* ORF were introduced by PCR primers and the *natNT2* cassette was amplified from *pFA6a–natNT2*.[44] The PCR product was transformed into YWY10 cells and colonies harboring successful recombination were selected on clonNAT plates and confirmed by genomic DNA PCR. The resulting strain was designated as YWY129.

Multicopy (2μ) suppressor screen

neo1-2 cells were transformed with 1 μg yeast genomic Tiling collection (GE, Dharmacon),[45] plated on SD-Leu plates and incubated at 37°C for 7–10 d. The surviving colonies were picked based on the colony size. The selected colonies were cultured at 30°C in suspension and plasmids were extracted. The mixed plasmids (pRS315-neo1-2 and a 2μ plasmid) from each colony were transformed into *E.coli*. and screened with kanamycin to select the 2μ plasmid. The 2μ plasmid was then sequenced to identify the inserted genomic DNA fragment. Recovered 2μ plasmids were also transformed back into *neo1-2* cells to confirm the suppression of *neo1-2* growth defect. The ORFs contained within the genomic DNA fragment with at least 500 bp upstream and 100 bp downstream sequences were amplified and individually cloned into pRS425 or pRS315. The resulting plasmids were transformed into *neo1-2* cells to identify *YPT7* as the ORF responsible for suppressing *neo1-2* growth defects at 37°C.

Vacuole staining

The vacuole staining using FM4-64 was performed as previously described.[46] Briefly, cells were shaken with 32 μM of endocytic dye FM4-64 (Life Technologies) for 20 min in the dark in YPD at 30°C, after which cells were harvested at 5,000 rpm for 1 minute, then re-suspended in YPD and incubated with shaking for 60 min at 30°C. Cells were subsequently washed twice in phosphate buffered saline (PBS) containing 2% glucose before visualization. For vacuole quantification in cells with no or moderately fragmented vacuoles, about 100 cells were randomly selected. Total cell number and total recognizable vacuole number inside these cells were counted and the average vacuole number per cell was defined as total vacuole number divided by total cell number. This process was repeated 3 times for each strain. For vacuole quantification in cells with highly fragmented vacuoles, vacuole number per cell in a cell population was classified into 2 categories: cells with 1-4 vacuoles and cells with 5 or more vacuoles. Any cells with distinct FM4-64 staining but too many vacuoles to reliably count were classified into cells with 5 or more vacuoles.

Fluorescence microscopy

Cells were washed twice with PBS containing 2% glucose before imaging. Images were acquired on a Zeiss AxioPlan scope using a 63× Plan-ApoChromat oil DIC objective (NA 1.40). A Cy3

or FITC filter was use for visualizing FM4-64 and DsRED or GFP respectively. Images were analyzed using ImageJ.

Western blots

Lysates from 0.1 OD_{600} of cells were subjected to SDS-gel electrophoresis. Western blot analysis was performed using Rabbit anti-Ypt7 (1:1000) and mouse anti-α-tubulin (1:4000) antibodies. Secondary antibodies were used at a 1:3000 dilution. Membranes were scanned at 800 nm and 680 nm simultaneously using the Odyssey Infrared Imaging System. Median band intensities were quantified using the Odyssey software (LI-COR Biosciences).

Disclosure of potential conflicts of interest

No potential conflicts of interest were disclosed.

Acknowledgments

We thank Bill Wickner for antibodies to Ypt7, and Chris Burd for the mKate strains and the DsRED-FYVE construct. We also thank Aki Nakano for the Rer1-GFP construct and Scott Moye-Rowley for the *psd* mutants.

Funding

This work was supported by grant GM107978 from the National Institutes of Health to T.R.G..

References

[1] Hankins HM, Baldridge RD, Xu P, Graham TR. Role of flippases, scramblases and transfer proteins in phosphatidylserine subcellular distribution. Traffic 2015; 16(1):35-47; PMID:25284293; http://dx.doi.org/10.1111/tra.12233

[2] Sebastian TT, Baldridge RD, Xu P, Graham TR. Phospholipid flippases: building asymmetric membranes and transport vesicles. Biochim Biophys Acta 2012; 1821(8):1068-77; PMID:22234261; http://dx.doi.org/10.1016/j.bbalip.2011.12.007

[3] Schroit AJ, Zwaal RF. Transbilayer movement of phospholipids in red cell and platelet membranes. Biochim Biophys Acta 1991; 1071(3):313-29; PMID:1958692; http://dx.doi.org/10.1016/0304-4157(91)90019-S

[4] Coleman JA, Kwok MC, Molday RS. Localization, purification, and functional reconstitution of the P4-ATPase Atp8a2, a phosphatidylserine flippase in photoreceptor disc membranes. J Biol Chem 2009; 284(47):32670-9; PMID:19778899; http://dx.doi.org/10.1074/jbc.M109.047415

[5] Zhou X, Graham TR. Reconstitution of phospholipid translocase activity with purified Drs2p, a type-IV P-type ATPase from budding yeast. Proc Natl Acad Sci U S A 2009; 106(39):16586-91; PMID:19805341; http://dx.doi.org/10.1073/pnas.0904293106

[6] Lopez-Marques RL, Poulsen LR, Bailly A, Geisler M, Pomorski TG, Palmgren MG. Structure and mechanism of ATP-dependent phospholipid transporters. Biochim Biophys Acta 2015; 1850(3):461-75; PMID:24746984; http://dx.doi.org/10.1016/j.bbagen.2014.04.008

[7] Coleman JA, Quazi F, Molday RS. Mammalian P4-ATPases and ABC transporters and their role in phospholipid transport. Biochim Biophys Acta 2013; 1831(3):555-74; PMID:23103747; http://dx.doi.org/10.1016/j.bbalip.2012.10.006

[8] Bevers EM, Williamson PL. Getting to the Outer Leaflet: Physiology of Phosphatidylserine Exposure at the Plasma Membrane. Physiol Rev 2016; 96(2):605-45; PMID:26936867; http://dx.doi.org/10.1152/physrev.00020.2015

[9] Suzuki J, Denning DP, Imanishi E, Horvitz HR, Nagata S. Xk-related protein 8 and CED-8 promote phosphatidylserine exposure in apoptotic cells. Science 2013; 341(6144):403-6; PMID:23845944; http://dx.doi.org/10.1126/science.1236758

[10] Suzuki J, Umeda M, Sims PJ, Nagata S. Calcium-dependent phospholipid scrambling by TMEM16F. Nature 2010; 468(7325):834-8; PMID:21107324; http://dx.doi.org/10.1038/nature09583

[11] Hua Z, Fatheddin P, Graham TR. An essential subfamily of Drs2p-related P-type ATPases is required for protein trafficking between Golgi complex and endosomal/vacuolar system. Mol Biol Cell 2002; 13(9):3162-77; PMID:12221123; http://dx.doi.org/10.1091/mbc.E02-03-0172

[12] Hua Z, Graham TR. Requirement for neo1p in retrograde transport from the Golgi complex to the endoplasmic reticulum. Mol Biol Cell 2003; 14(12):4971-83; PMID:12960419; http://dx.doi.org/10.1091/mbc.E03-07-0463

[13] Huh WK, Falvo JV, Gerke LC, Carroll AS, Howson RW, Weissman JS, O'Shea EK. Global analysis of protein localization in budding yeast. Nature 2003; 425(6959):686-91; PMID:14562095; http://dx.doi.org/10.1038/nature02026

[14] Wicky S, Schwarz H, Singer-Kruger B. Molecular interactions of yeast Neo1p, an essential member of the Drs2 family of aminophospholipid translocases, and its role in membrane trafficking within the endomembrane system. Mol Cell Biol 2004; 24(17):7402-18; PMID:15314152; http://dx.doi.org/10.1128/MCB.24.17.7402-7418.2004

[15] Takatsu H, Baba K, Shima T, Umino H, Kato U, Umeda M, Nakayama K, Shin HW. ATP9B, a P4-ATPase (a putative aminophospholipid translocase), localizes to the trans-Golgi network in a CDC50 protein-independent manner. J Biol Chem 2011; 286(44):38159-67; PMID:21914794; http://dx.doi.org/10.1074/jbc.M111.281006

[16] Wehman AM, Poggioli C, Schweinsberg P, Grant BD, Nance J. The P4-ATPase TAT-5 inhibits the budding of extracellular vesicles in C. elegans embryos. Curr Biol 2011; 21(23):1951-9; PMID:22100064

[17] Takar M, Wu Y, Graham TR. The essential Neo1 from budding yeast plays a role in establishing aminophospholipid asymmetry of the plasma membrane. J Biol Chem 2016; 291:15727-39; PMID:27235400

[18] Brett CL, Kallay L, Hua Z, Green R, Chyou A, Zhang Y, Graham TR, Donowitz M, Rao R. Genome-wide analysis reveals the vacuolar pH-stat of Saccharomyces cerevisiae. PloS one 2011; 6(3):e17619; PMID:21423800; http://dx.doi.org/10.1371/journal.pone.0017619

[19] Wickner W. Membrane fusion: five lipids, four SNAREs, three chaperones, two nucleotides, and a Rab, all dancing in a ring on yeast vacuoles. Ann Rev Cell Dev Biol 2010; 26:115-36; PMID:20521906; http://dx.doi.org/10.1146/annurev-cellbio-100109-104131

[20] Hickey CM, Stroupe C, Wickner W. The major role of the Rab Ypt7p in vacuole fusion is supporting HOPS membrane association. J Biol Chem 2009; 284(24):16118-25; PMID:19386605; http://dx.doi.org/10.1074/jbc.M109.000737

[21] Wang L, Seeley ES, Wickner W, Merz AJ. Vacuole fusion at a ring of vertex docking sites leaves membrane fragments within the organelle. Cell 2002; 108(3):357-69; PMID:11853670; http://dx.doi.org/10.1016/S0092-8674(02)00632-3

[22] Mima J, Hickey CM, Xu H, Jun Y, Wickner W. Reconstituted membrane fusion requires regulatory lipids, SNAREs and synergistic SNARE chaperones. EMBO J 2008; 27(15):2031-42; PMID:18650938; http://dx.doi.org/10.1038/emboj.2008.139

[23] Stroupe C, Collins KM, Fratti RA, Wickner W. Purification of active HOPS complex reveals its affinities for phosphoinositides and the SNARE Vam7p. EMBO J 2006; 25(8):1579-89; PMID:16601699; http://dx.doi.org/10.1038/sj.emboj.7601051

[24] Mima J, Wickner W. Complex lipid requirements for SNARE- and SNARE chaperone-dependent membrane fusion. J Biol Chem 2009; 284(40):27114-22; PMID:19654322; http://dx.doi.org/10.1074/jbc.M109.010223

[25] Zick M, Stroupe C, Orr A, Douville D, Wickner WT. Membranes linked by trans-SNARE complexes require lipids prone to non-

bilayer structure for progression to fusion. eLife 2014; 3:e01879; PMID:24596153

[26] Jun Y, Fratti RA, Wickner W. Diacylglycerol and its formation by phospholipase C regulate Rab- and SNARE-dependent yeast vacuole fusion. J Biol Chem 2004; 279(51):53186-95; PMID:15485855; http://dx.doi.org/10.1074/jbc.M411363200

[27] Seeley ES, Kato M, Margolis N, Wickner W, Eitzen G. Genomic analysis of homotypic vacuole fusion. Mol Biol Cell 2002; 13(3):782-94; PMID:11907261; http://dx.doi.org/10.1091/mbc.01-10-0512

[28] Fratti RA, Jun Y, Merz AJ, Margolis N, Wickner W. Interdependent assembly of specific regulatory lipids and membrane fusion proteins into the vertex ring domain of docked vacuoles. J Cell Biol 2004; 167(6):1087-98; PMID:15611334; http://dx.doi.org/10.1083/jcb.200409068

[29] Keenan Curtis K, Kane PM. Novel vacuolar H+-ATPase complexes resulting from overproduction of Vma5p and Vma13p. J Biol Chem 2002; 277(4):2716-24; PMID:11717306; http://dx.doi.org/10.1074/jbc.M107777200

[30] Haas A, Scheglmann D, Lazar T, Gallwitz D, Wickner W. The GTPase Ypt7p of Saccharomyces cerevisiae is required on both partner vacuoles for the homotypic fusion step of vacuole inheritance. EMBO J 1995; 14(21):5258-70; PMID:7489715

[31] Mumberg D, Muller R, Funk M. Yeast vectors for the controlled expression of heterologous proteins in different genetic backgrounds. Gene 1995; 156(1):119-22; PMID:7737504; http://dx.doi.org/10.1016/0378-1119(95)00037-7

[32] Wood CS, Hung CS, Huoh YS, Mousley CJ, Stefan CJ, Bankaitis V, Ferguson KM, Burd CG. Local control of phosphatidylinositol 4-phosphate signaling in the Golgi apparatus by Vps74 and Sac1 phosphoinositide phosphatase. Mol Biol Cell 2012; 23(13):2527-36; PMID:22553352; http://dx.doi.org/10.1091/mbc.E12-01-0077

[33] Katzmann DJ, Stefan CJ, Babst M, Emr SD. Vps27 recruits ESCRT machinery to endosomes during MVB sorting. J Cell Biol 2003; 162(3):413-23; PMID:12900393; http://dx.doi.org/10.1083/jcb.200302136

[34] Baldridge RD, Graham TR. Identification of residues defining phospholipid flippase substrate specificity of type IV P-type ATPases. Proc Natl Acad Sci U S A 2012; 109(6):E290-8; PMID:22308393; http://dx.doi.org/10.1073/pnas.1115725109

[35] Sato K, Sato M, Nakano A. Rer1p, a retrieval receptor for endoplasmic reticulum membrane proteins, is dynamically localized to the Golgi apparatus by coatomer. J Cell Biol 2001; 152(5):935-44; PMID:11238450; http://dx.doi.org/10.1083/jcb.152.5.935

[36] Birner R, Burgermeister M, Schneiter R, Daum G. Roles of phosphatidylethanolamine and of its several biosynthetic pathways in Saccharomyces cerevisiae. Mol Biol Cell 2001; 12(4):997-1007; PMID:11294902; http://dx.doi.org/10.1091/mbc.12.4.997

[37] Gulshan K, Shahi P, Moye-Rowley WS. Compartment-specific synthesis of phosphatidylethanolamine is required for normal heavy metal resistance. Mol Biol Cell 2010; 21(3):443-55; PMID:20016005; http://dx.doi.org/10.1091/mbc.E09-06-0519

[38] Alder-Baerens N, Lisman Q, Luong L, Pomorski T, Holthuis JC. Loss of P4 ATPases Drs2p and Dnf3p disrupts aminophospholipid transport and asymmetry in yeast post-Golgi secretory vesicles. Mol Biol Cell 2006; 17(4):1632-42; PMID:16452632; http://dx.doi.org/10.1091/mbc.E05-10-0912

[39] Natarajan P, Wang J, Hua Z, Graham TR. Drs2p-coupled aminophospholipid translocase activity in yeast Golgi membranes and relationship to in vivo function. Proc Natl Acad Sci U S A 2004; 101(29):10614-9; PMID:15249668; http://dx.doi.org/10.1073/pnas.0404146101

[40] Liu K, Hua Z, Nepute JA, Graham TR. Yeast P4-ATPases Drs2p and Dnf1p are essential cargos of the NPFXD/Sla1p endocytic pathway. Mol Biol Cell 2007; 18(2):487-500; PMID:17122361; http://dx.doi.org/10.1091/mbc.E06-07-0592

[41] Liu K, Surendhran K, Nothwehr SF, Graham TR. P4-ATPase requirement for AP-1/clathrin function in protein transport from the trans-Golgi network and early endosomes. Mol Biol Cell 2008; 19(8):3526-35; PMID:18508916; http://dx.doi.org/10.1091/mbc.E08-01-0025

[42] Mima J, Wickner W. Phosphoinositides and SNARE chaperones synergistically assemble and remodel SNARE complexes for membrane fusion. Proc Natl Acad Sci U S A 2009; 106(38):16191-6; PMID:19805279; http://dx.doi.org/10.1073/pnas.0908694106

[43] Hua ZL, Graham TR. Requirement for Neo1p in retrograde transport from the Golgi complex to the endoplasmic reticulum. Mol Biol Cell 2003; 14(12):4971-83; PMID:12960419; http://dx.doi.org/10.1091/mbc.E03-07-0463

[44] Janke C, Magiera MM, Rathfelder N, Taxis C, Reber S, Maekawa H, Moreno-Borchart A, Doenges G, Schwob E, Schiebel E, et al. A versatile toolbox for PCR-based tagging of yeast genes: new fluorescent proteins, more markers and promoter substitution cassettes. Yeast 2004; 21(11):947-62; PMID:15334558; http://dx.doi.org/10.1002/yea.1142

[45] Jones GM, Stalker J, Humphray S, West A, Cox T, Rogers J, Dunham I, Prelich G. A systematic library for comprehensive overexpression screens in Saccharomyces cerevisiae. Nat Methods 2008; 5(3):239-41; PMID:18246075; http://dx.doi.org/10.1038/nmeth.1181

[46] Vida TA, Emr SD. A new vital stain for visualizing vacuolar membrane dynamics and endocytosis in yeast. J Cell Biol 1995; 128(5):779-92; PMID:7533169; http://dx.doi.org/10.1083/jcb.128.5.779

[47] Katzmann DJ, Stefan CJ, Babst M, Emr SD. Vps27 recruits ESCRT machinery to endosomes during MVB sorting. J Cell Biol 2003; 162(3):413-23; PMID:12900393; http://dx.doi.org/10.1083/jcb.200302136

[48] Sato K, Sato M, Nakano A. Rer1p, a retrieval receptor for endoplasmic reticulum membrane proteins, is dynamically localized to the Golgi apparatus by coatomer. J Cell Biol 2001; 152(5):935-44; PMID:11238450; http://dx.doi.org/10.1083/jcb.152.5.935

[49] Wood CS, Hung CS, Huoh YS, Mousley CJ, Stefan CJ, Bankaitis V, Ferguson KM, Burd CG. Local control of phosphatidylinositol 4-phosphate signaling in the Golgi apparatus by Vps74 and Sac1 phosphoinositide phosphatase. Mol Biol Cell 2012; 23(13):2527-36; PMID:22553352; http://dx.doi.org/10.1091/mbc.E12-01-0077

[50] Gulshan K, Schmidt JA, Shahi P, Moye-Rowley WS. Evidence for the bifunctional nature of mitochondrial phosphatidylserine decarboxylase: role in Pdr3-dependent retrograde regulation of PDR5 expression. Mol Cell Biol 2008; 28(19):5851-64; PMID:18644857; http://dx.doi.org/10.1128/MCB.00405-08